INSTITUTE OF PHYSICS PUBLISHING JOURNAL OF OPTICS A: PURE AND APPLIED OPTICS

J. Opt. A: Pure Appl. Opt. **9** (2007) 81–87 doi:10.1088/1464-4258/9/1/014

Coupling of evanescent s-polarized waves to the far field by waveguide modes in metallic arrays

Marcelo Lester[1,3] **and Diana C Skigin**[2,3]

[1] Instituto de Física Arroyo Seco, Facultad de Ciencias Exactas, Universidad Nacional del Centro de la Provincia de Buenos Aires, Pinto 399 (cp 7000) Buenos Aires, Argentina
[2] Grupo de Electromagnetismo Aplicado, Departamento de Física, Facultad de Ciencias Exactas y Naturales, Universidad de Buenos Aires, Ciudad Universitaria, Pabellón I, C1428EHA Buenos Aires, Argentina

Received 1 September 2006, accepted for publication 3 November 2006
Published 28 November 2006
Online at stacks.iop.org/JOptA/9/81

Abstract
In this paper we show that enhanced optical transmission through a 1D periodic slit array comprising real metallic cylinders is possible for s-polarization when the array is near a dielectric interface. We investigate the behaviour of this structure under s-polarized illumination, in which case surface plasmons are not excited. Numerical results show that the transmitted intensity appears as a periodic function of the slit depth, for propagating as well as for evanescent incidence, suggesting that this behaviour is related to the excitation of waveguide modes in the slits. In particular, the coupling of evanescent to propagating electromagnetic waves is investigated. It is shown that s-polarized evanescent waves generated at the interface can be transformed into propagating waves if the optical width of the slits allows propagation of the first waveguide mode. As the interface approaches the array, the transmitted intensity increases for evanescent incidence.

Keywords: grating-waveguide structures, resonances, anomaly, enhanced transmission

1. Introduction

Since the report of extraordinary optical transmission (EOT), first published by Ebbesen *et al* [1], many works have been devoted to deeply understand the origin of such a phenomenon, and the physics involved in the excitation of resonant modes in periodic structures. In particular, 1D structures formed by an array of metallic cylinders have been widely studied [2–7]. The mechanisms identified as responsible for the field enhancement are (i) the excitation of surface waves or eigenmodes of the structure, and (ii) Fabry–Perot resonances in subwavelength slits. Surface waves are electromagnetic fields that propagate parallel to the interface and whose amplitudes are exponentially decaying in the normal direction [8, 9], and which can be found in metal–dielectric interfaces, in which case they are identified as surface plasmons [10–12], as well as in dielectric–dielectric interfaces [13] or recently, spoof plasmons in a perfect conductor [14]. Waveguide or Fabry–Perot resonances, on the other hand, are originated by constructive interference of multiple reflections into each nano- or micro-cavity, and a periodic array of narrow slits (grating) acts as an amplifier of these individual resonances [2, 3, 8].

The resonant coupling between the incident radiation and the different eigenmodes supported by the structure gives rise to a large variety of electromagnetic effects, some of which have already concrete technological applications in near-field microscopy [15, 16], imaging [17, 18], medical diagnostics [19, 20], optical communications and computing. Most of the studies involving metallic structures are based on the excitation of surface plasmon polaritons, which can only be excited in 1D structures if illuminated by a p-polarized wave [17, 18, 21–24]. However, Moreno *et al* recently showed that extraordinary optical transmission is possible even for s-polarization [25].

In a previous paper we reported numerical evidence of an efficient coupling between the incident evanescent wave and

[3] Consejo Nacional de Investigaciones Científicas y Técnicas CONICET.

the far-field transmitted wave in structures formed by an array of rectangular metallic wires near a dielectric interface [26]. This coupling was helped by the excitation of surface plasmon polaritons.

In this paper we show that it is possible to get enhanced optical transmission through metallic subwavelength slits for s-polarized illumination, in the absence of surface plasmons. We investigate the possibility of transforming an evanescent s-polarized plane wave into a far-field transmitted wave by means of a 1D metallic array. At present, the evanescent-to-propagating wave conversion for s-polarization has technological interest in solid state light-emitting diodes (LEDs). It was recently shown that the influence of spatial effects induces self-sustained oscillations of the total laser output and a sudden change of the linear polarization can be self-stimulated (for instance, from s- to p-polarization) [27–29]. In these devices, the relative refractive index between the external LEDs face and air is larger than 1 and, due to the existence of a critical angle, only a narrow light cone emerges from the LED. The internally reflected light is reabsorbed by active layers or electrodes, thus diminishing its efficiency. Then, it would be interesting to have a structure that can couple light to the far field regardless of the polarization mode.

We use the modal method to solve the diffraction problem from a periodic array of rectangular wires [26]. This method is particularly suitable for rectangular geometries of the scatterers, and has been successfully applied in many diffraction and scattering problems [30–32]. We also consider a structure formed by a finite array of metallic circular cylinders, and the solution of this scattering problem is found using an integral method based on the extinction theorem [33]. The dependence of the transmitted intensity on the thickness of the wires, on the width of the slits, on the distance to the dielectric interface and on the angle of incidence are studied. Finally, the conclusions are given.

2. Configuration and methods of resolution

In this section we explain the configurations of the problems considered in this paper and summarize the methods employed for their resolutions.

2.1. Infinite array: modal approach

We consider an infinitely periodic array of rectangular metallic wires near a dielectric interface (see figure 1(a)). The interface plane at $y = 0$ separates two isotropic dielectric non-magnetic media ($\mu = 1$). The lower region (region 1) has a permittivity ε_1; the periodic array is immersed in air ($\varepsilon_0 = 1$), and is at a distance e from the interface. The period of the structure is d and the metallic wires have a rectangular cross section of side h and a complex dielectric constant ε_2. The system is illuminated from $y < 0$ by a plane wave of wavelength λ_0 in vacuum, forming an angle θ_1 with the y axis. Since we consider an incidence wavevector contained in the main section of the structure (the (x, y) plane), the vectorial problem can be separated into two scalar problems corresponding to the polarization modes: s (electric field perpendicular to the incidence plane) and p (electric field parallel to the incidence plane). The diffraction problem is solved separately for

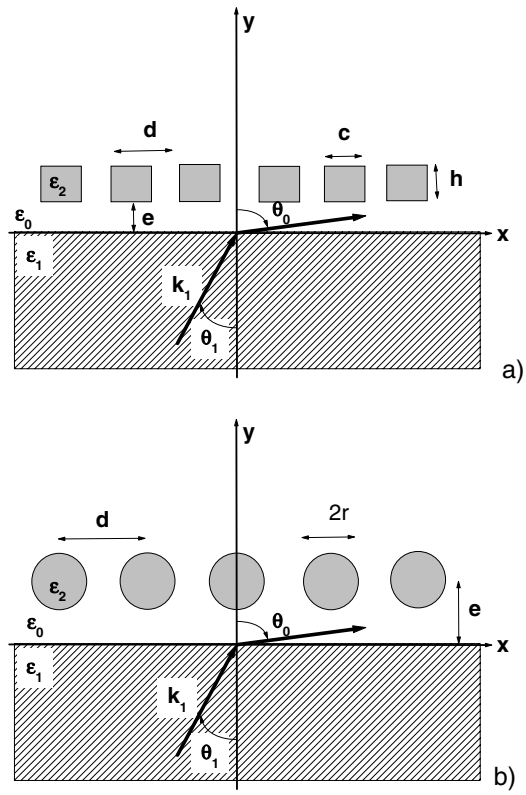

Figure 1. Geometries of the systems considered: different metallic arrays near a dielectric interface. (a) Infinite periodic array of rectangular wires; (b) finite array of circular cylinders.

each polarization mode using the modal method for highly conducting wire gratings [31], extended to allow additional dielectric interfaces.

The method consists in dividing the spatial domain into regions, and expanding the fields in each region into its own eigenfunctions. In this case, the four regions are separated by the horizontal interfaces at $y = 0$, $y = e$, and $y = e + h$. In the region $y \leqslant 0$ we have the incident plane wave and the reflected field and in $y \geqslant e + h$ we have the transmitted field. The outgoing fields (reflected and transmitted) are represented by sums of outgoing plane waves with unknown complex amplitudes. In the layer between the interface and the array ($0 \leqslant y \leqslant e$), the field is represented by a combination of up and down plane waves, and inside the slits ($e \leqslant y \leqslant e + h$), the fields are expanded in terms of eigenfunctions that take into account the surface impedance boundary condition (SIBC) on the lateral walls of each slit [31]. The fields are matched at the horizontal interfaces by imposing the continuity of the tangential components in the open sections, and by applying the SIBC in the metallic regions. The resulting equations are projected in convenient bases, which leads to a system of coupled equations that can be put in matrix form, which has to be solved for the unknown reflected and transmitted amplitudes. More details on this formulation are given in [26].

2.2. Finite array: integral method

We consider a finite array of N metallic cylinders of radius r and circular cross section bounded by a contour C, distributed

periodically with period d (see figure 1(b)). As in the previous configuration, the array is immersed in vacuum, and is near a dielectric interface whose surface profile is described by the function $y = D$. In this case, the distance e between the cylinders and the interface is measured from the centre of the cylinders. A Gaussian incident beam of half-width W is considered, which can simulate a plane wave by setting W sufficiently large.

To compute the near and far field, we implemented a rigorous method based on the extinction theorem (ET) for multiply connected domains [34]. The advantage that these methods have over other approaches stems from their complete generality regardless of the geometry of the scattering surface or its constitutive parameters, which makes them very suitable for simulating scattering processes.

In what follows we summarize the ET method applied to 2D systems, as is the case of the present study.

For systems with translation symmetry (2D geometries), the expressions for the scattered field in each medium are:

$$\begin{aligned}\phi_\alpha^{(0)}(\mathbf{r}) = \frac{\mathrm{i}}{4}\int_{D^{(+)}} \mathrm{d}l' \Bigg[& \frac{\partial H_0^{(1)}(\sqrt{\varepsilon_0}k_0|\mathbf{r}-\mathbf{r}'|)}{\partial \mathbf{n}'}\phi_\alpha^{(0)}(\mathbf{r}') \\ & - H_0^{(1)}(\sqrt{\varepsilon_0}k_0|\mathbf{r}-\mathbf{r}'|)\frac{\partial \phi_\alpha^{(0)}(\mathbf{r}')}{\partial \mathbf{n}'}\Bigg] \\ & + \sum_{j=2}^{M}\Bigg\{\frac{\mathrm{i}}{4}\int_{C_j^{(+)}} \mathrm{d}l' \Bigg[\frac{\partial H_0^{(1)}(\sqrt{\varepsilon_0}k_0|\mathbf{r}-\mathbf{r}'|)}{\partial \mathbf{n}'}\phi_\alpha^{(0)}(\mathbf{r}') \\ & - H_0^{(1)}(\sqrt{\varepsilon_0}k_0|\mathbf{r}-\mathbf{r}'|)\frac{\partial \phi_\alpha^{(0)}(\mathbf{r}')}{\partial \mathbf{n}'}\Bigg]\Bigg\},\end{aligned} \tag{1}$$

$$\begin{aligned}\phi_\alpha^{(1)}(\mathbf{r}) = {} & \phi_\alpha^{(\mathrm{inc})}(\mathbf{r}) \\ & - \frac{\mathrm{i}}{4}\int_{D^{(-)}} \mathrm{d}l' \Bigg[\frac{\partial H_0^{(1)}(\sqrt{\varepsilon_1}k_0|\mathbf{r}-\mathbf{r}'|)}{\partial \mathbf{n}'}\phi_\alpha^{(1)}(\mathbf{r}') \\ & - H_0^{(1)}(\sqrt{\varepsilon_1}k_0|\mathbf{r}-\mathbf{r}'|)\frac{\partial \phi_\alpha^{(1)}(\mathbf{r}')}{\partial \mathbf{n}'}\Bigg],\end{aligned} \tag{2}$$

$$\begin{aligned}\phi_\alpha^{(j)}(\mathbf{r}) = -\frac{\mathrm{i}}{4\pi}\int_{C_j^{(-)}} \mathrm{d}l' \Bigg[& \frac{\partial H_0^{(1)}(\sqrt{\varepsilon_j}k_0|\mathbf{r}-\mathbf{r}'|)}{\partial \mathbf{n}'}\phi_\alpha^{(j)}(\mathbf{r}') \\ & - H_0^{(1)}(\sqrt{\varepsilon_j}k_0|\mathbf{r}-\mathbf{r}'|)\frac{\partial \phi_\alpha^{(j)}(\mathbf{r}')}{\partial \mathbf{n}'}\Bigg]; \\ & \text{for } j = 2, \ldots, M,\end{aligned} \tag{3}$$

where $\phi_\alpha^{(j)}(\mathbf{r})$ represents the complex amplitudes of the electric ($\alpha = \mathrm{s}$) or the magnetic ($\alpha = \mathrm{p}$) field in the host medium ($j = 0$), in the incident medium ($y \leqslant 0$, $j = 1$), or within any of the N scatterers ($j = 2, \ldots, M$); $\mathrm{d}l'$ is a differential element of line over the contour C_j or D. The superscript $^{(+)}$ in $D^{(+)}$ denotes that the integration is done over the contour D for the integration variable $\mathbf{r}'$ approaching this boundary from the host medium ($j = 0$), the normal vector $\mathbf{n}'$ points towards the interior of this medium. D^- denotes that the variable $\mathbf{r}'$ approaches D from the incident medium ($j = 1$) and the normal vector $\mathbf{n}'$ points towards the interior of this medium. In similar form $C_j^{(+)}$ represents the cross section contour of the jth scatterer when $\mathbf{r}'$ tends to C_j from the host medium, and in this case $\mathbf{n}'$ points towards the interior of the jth medium. Conversely, $C_j^{(-)}$ represents the cross section contour of the jth scatterer when $\mathbf{r}'$ tends to C_j from the interior of the jth medium, and $\mathbf{n}'$ points outwards of the jth medium. $H_0^{(1)}$ is the first class zero-order Hankel function.

In 2D problems, the boundary conditions reduce to two separate pairs of equations, for s and p modes:

$$\left[\phi_\alpha^{(0)}(\mathbf{r})\right]_{\mathbf{r}\in C_j^{(+)}} = \left[\phi_\alpha^{(j)}(\mathbf{r})\right]_{\mathbf{r}\in C_j^{(-)}} \tag{4}$$

$$\left[\frac{\partial \phi_\alpha^{(0)}(\mathbf{r})}{\partial \mathbf{n}'}\right]_{\mathbf{r}\in C_j^{(+)}} = \left[\eta_j(\alpha)\frac{\partial \phi_\alpha^{(j)}(\mathbf{r})}{\partial \mathbf{n}'}\right]_{\mathbf{r}\in C_j^{(-)}}, \tag{5}$$

with $j = 1, 2, \ldots, M$ and $\eta_j(\mathrm{s}) = \mu_j/\mu_0$, $\eta_j(\mathrm{p}) = \varepsilon_j/\varepsilon_0$. Equations (4) and (5) do not couple polarization modes, which implies that in a 2D system there is no cross-polarization.

To compute the far field in the forward direction, we obtain the expression for the transmitted far field from the previous equations making use of the asymptotic expression for the Hankel function when $|\mathbf{r}-\mathbf{r}'| \to \infty$:

$$\begin{aligned}\phi_\alpha^{(t)}(r,\theta_t) = {} & \frac{\exp\left[\mathrm{i}\sqrt{\varepsilon_0}k_0 r - \pi/4\right]}{\sqrt{8\pi(\varepsilon_0)^{1/2}k_0 r}} \\ & \times \Bigg\{\int_{D^{(+)}} \mathrm{d}l' \left((\mathbf{n}'\cdot\mathbf{k}_t)\phi_\alpha^{(0)}(\mathbf{r}') - \mathrm{i}\frac{\partial \phi_\alpha^{(0)}(\mathbf{r}')}{\partial \mathbf{n}'}\right) \\ & \times \exp(-\mathrm{i}\mathbf{k}_t\cdot\mathbf{r}) + \sum_{j=1}^{N}\Bigg[\int_{C_j^{(+)}} \mathrm{d}l' \Bigg((\mathbf{n}'\cdot\mathbf{k}_t)\phi_\alpha^{(0)}(\mathbf{r}') \\ & - \mathrm{i}\frac{\partial \phi_\alpha^{(0)}(\mathbf{r}')}{\partial \mathbf{n}'}\Bigg)\exp(-\mathrm{i}\mathbf{k}_t\cdot\mathbf{r})\Bigg]\Bigg\},\end{aligned} \tag{6}$$

where $\mathbf{k}_t$ is the propagation vector, defined by

$$\mathbf{k}_t = \sqrt{\varepsilon_0}k_0(\sin\theta_t, 0, \cos\theta_t), \tag{7}$$

and θ_t is the observation angle. The incident field appears in implicit form in the scattering equations.

3. Results

In figure 2 we show maps of total transmitted intensity as a function of the incidence angle θ_1. The structure is illuminated from the dielectric medium by a plane wave of wavelength $\lambda_0 = 717$ nm (the refraction index of silver at this wavelength is $\nu = 0.146 + \mathrm{i}4.64$). Rectangular silver wires of thickness h are ordered in a periodic array of period $d = 1.13\lambda_0$; the array is located at a distance $e = 0.25\lambda_0$ from the interface that separates the vacuum from the incidence medium ($\varepsilon_1 = 2.25$). Two wire widths are considered: $c = 0.56\lambda_0$ (figures 2(a) and (b)) and $c = 0.7\lambda_0$ (figures 2(c) and (d)). For these two cases, the slit widths are $a = 0.577\lambda_0$ and $a = 0.438\lambda_0$, respectively.

In general, for a parallel plate perfectly conducting waveguide, the first mode allowed for s-polarization (in the x direction) is such that $a = \lambda_0/2$. Then, for $a < \lambda_0/2$ there are no modes propagating through the slits, and no transmission should be expected. On the other hand, there is no limitation in the slit width for the propagation of p-waves within the waveguide, and therefore some transmission could be expected even for very narrow slits for this polarization.

Figures 2(a) and (c) correspond to s-polarization and figures 2(b) and (d) to p-polarization. The critical angle for this dielectric interface is $\theta_c = 41.8°$, which implies that for $\theta_1 > \theta_c$ the wave that arrives at the metallic array is an evanescent wave. In all four maps a clear vertical line exactly at

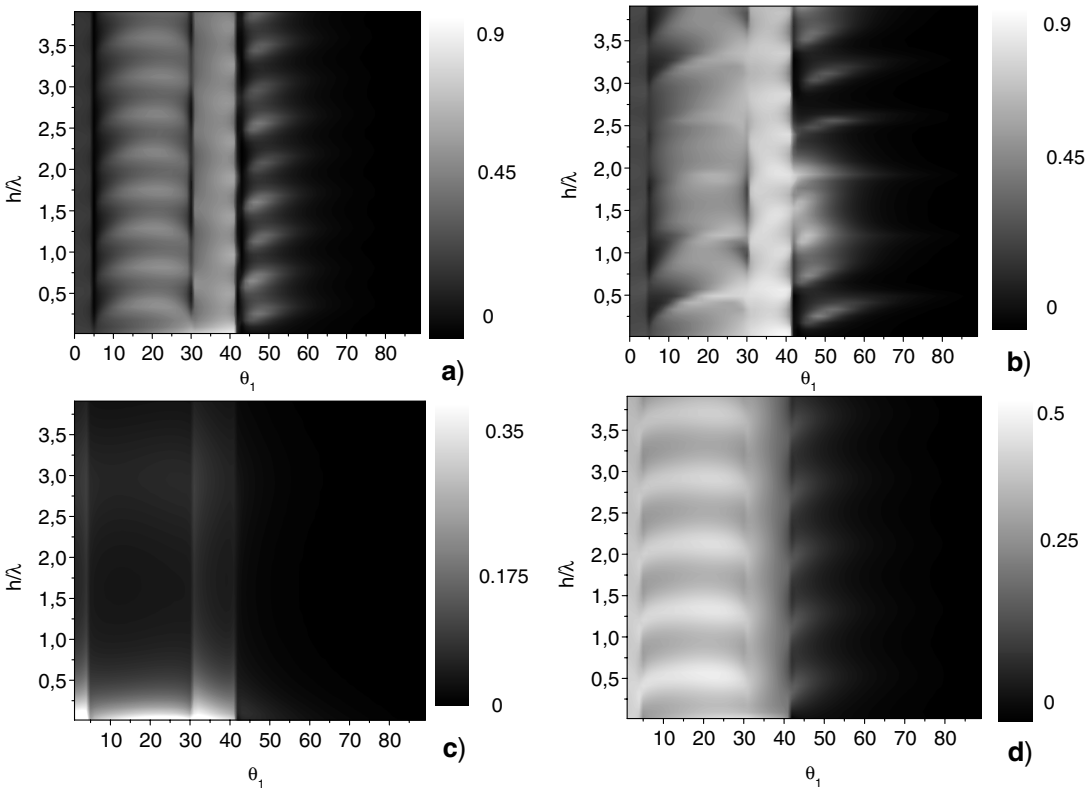

Figure 2. Maps of total transmitted intensity as a function of the incidence angle θ_1 and of h/λ_0 for a periodic array of silver wires. $d = 814$ nm, $e = 179.25$ nm, $\varepsilon_1 = 2.25$, $\lambda_0 = 717$ nm and $\nu_2 = 0.146 + \mathrm{i}4.64$. (a) $c = 400$ nm and s-polarization; (b) $c = 400$ nm and p-polarization; (c) $c = 500$ nm and s-polarization; (d) $c = 500$ nm and p-polarization.

$\theta_1 = \theta_c$ can be appreciated, and it is also possible to distinguish two vertical lines at $\theta_1 = 4.6°$ and $30.4°$, which correspond to the incidence angles at which the $+1$ order disappears and the -2 order appears, respectively. In most cases the transmitted intensity is significantly higher for $\theta_1 < \theta_c$, i.e. when the wave incident on the array is propagating.

In figures 2(a) and (b), however, there are certain values of h/λ_0 for which there is quite an important transmission rate for evanescent incidence as well. For s-polarization, the maximum transmission for evanescent incidence is about 30% of the incoming power, whereas for p-polarization the transmission reaches up to 70% (see figure 2(b)). The difference between both polarization modes is due to the excitation of a surface plasmon polariton (SPP) that enhances the transmission in the p-case [26]. Even though for s-polarization SPPs are not excited, several transmission maxima are obtained (see figure 2(a)). These maxima appear nearly equally spaced in h/λ_0, with a period $w \approx 0.8$. For other thicknesses, the transmission is negligible. This periodicity in h/λ_0 led us to think that the intensification of the transmitted efficiency is caused by geometrical eigenmodes, like Fabry–Perot resonances, excited in the slits.

The results shown in figures 2(c) and (d) correspond to the same system but for a larger wire width $c = 0.7\lambda_0$ (smaller slit width $a = 0.438\lambda_0$). For the s-case almost no transmission at the evanescent zone is observed, and for $h/\lambda_0 > 1.5$ the transmission is practically null for any incident angle. For the p-case, on the other hand, the map is qualitatively similar to figure 2(b).

To understand the behaviour of the transmission coefficient shown in figure 2(a), we assume that a Fabry–Perot resonance (FPR) happens within the slits. Therefore, if a FPR takes place, the wavelength of the electromagnetic field inside the slit should satisfy $h/\lambda^* = m/2$, with $m = 1, 2, 3, \ldots$. Here λ^* is the resonant Fabry–Perot wavelength and it can be expressed as $\lambda^* = \lambda_0/\nu_{\mathrm{eff}}$ with ν_{eff} being the effective refractive index inside the slit. This function ν_{eff} depends on a/λ_0 and is given by [35, 36]

$$\nu_{\mathrm{eff}}^{(n)} = \beta_n/k_0, \tag{8}$$

where β_n is the propagation constant of the nth mode along the slit. In figure 3 the evolution of the effective index for the first and second guided modes for the parameters of figures 2(a) and (c) (s-polarization) are shown. For $a = 0.577\lambda_0$, the effective refraction index is $\nu_{\mathrm{eff}\,1} = 0.632 + \mathrm{i}0.0031$. For $a = 0.438\lambda_0$, the effective index is $\nu_{\mathrm{eff}\,1} = 0.149 + \mathrm{i}0.027$, i.e. the first mode of the electromagnetic field is significantly damped and for large h/λ_0 no transmitted electromagnetic field can be expected throughout the slit, just as observed in figure 2(c).

To further investigate the origin of the evanescent-to-propagating coupling in the s-case, we performed calculations of the total transmitted efficiency as a function of the slit width a, shown in the maps of figure 4 for the same system of figure 2 but for a fixed thickness $h = 0.5\lambda_0$, and for two values of the array-to-interface distance e. It is clear from these maps that no transmission is found for slit widths smaller than $0.46\lambda_0$ for all incidence angles. For $a > 0.46\lambda_0$, transmission is

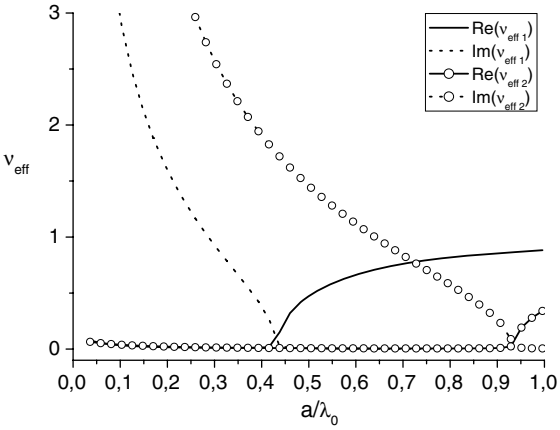

Figure 3. Effective refraction index of the first and second modes within the slits as a function of the slit width-to-wavelength ratio a/λ_0, for the same parameters of figures 2(a) and (c) (s-polarization).

found for propagating incidence, i.e. for $\theta_1 < \theta_c$, but for evanescent incidence the transmitted intensity depends on the distance between the metallic array and the interface. Whereas for $e = 0.25\lambda_0$ there is almost no evanescent coupling for $0.46 < a/\lambda_0 < 0.92$ (figure 4(a)), this coupling becomes very significant for $e = 0.014\lambda_0$, for all $a > 0.46\lambda_0$, even for very large incidence angles (figure 4(b)). It is also interesting to notice that, in figure 4(a), an increase in the evanescent-to-propagating coupling is found for $a \sim 0.98\lambda_0$. For this value of the slit width, the second waveguide mode within the slit becomes propagating, as can be observed in figure 3. This increases the coupling and consequently produces larger transmission to the far field. For instance, for $a = 1.06\lambda_0$, a 40% coupling is obtained for $\theta_1 \approx 50°$.

When the array is very close to the dielectric interface, the only existence of a single mode within the slits guarantees the coupling of evanescent to propagating waves (figure 4(b)). Each slit behaves like an evanescent electromagnetic field source located at the top of the array, and then a set of periodic sources is obtained at $y = e + h$. The sources are coupled by means of the periodicity of the system, i.e. if $\hat{\kappa} = \kappa/k_0 = \sin\theta\hat{x}$ is the normalized propagation constant of the evanescent field along the periodic system ($|\hat{\kappa}| > 1$), and $\vec{K} = (2\pi/d)\,\hat{x}$ is the momentum provided by the periodic array, then the propagation constant κ can be coupled to the periodicity of the system via a suitable momentum $\vec{K}$. The family of κ_n diffracted in the $\hat{x}$ direction is given by

$$\kappa_n = \kappa + nK. \tag{9}$$

Dividing equation (9) by k_0 and defining $\hat{\kappa}_n = \kappa_n/k_0$ we get

$$\hat{\kappa}_n = \hat{\kappa} + n\frac{\lambda_0}{d}. \tag{10}$$

If we identify $\hat{\kappa}_n$ with $\sin\theta_{0n}$ (angle of the nth diffracted order), equation (10) takes the form

$$\sin\theta_{0n} = \sqrt{\varepsilon_1}\sin\theta_1 + n\frac{\lambda_0}{d}, \tag{11}$$

and these orders are propagating orders if $(\cos\theta_{0n})^2 = \varepsilon_0 - (\sin\theta_{0n})^2 < 1$, regardless of the incident wave polarization. Then, the evanescent wave generated at the periodic array is diffracted and transmitted in certain particular directions.

The mechanism responsible for the enhanced transmission observed for angles of incidence $\theta_1 > \theta_c$ in figure 2(a) is exactly the same as that for propagating incidence: excitation of FPRs, and coupling of the damped vertical propagation constant and the periodic array (the array is close enough to the interface). Under this condition, a FPR can be stimulated and the near field is enhanced.

In the previous examples we have shown that, when an evanescent wave impinges on a periodic array of wires, it can be coupled to a propagating wave and transmitted to the far field. This effect is a result of two mechanisms that act simultaneously in this structure. The first one is produced by the periodicity of the array, which allows for transmitted diffraction orders in certain particular directions. This fact

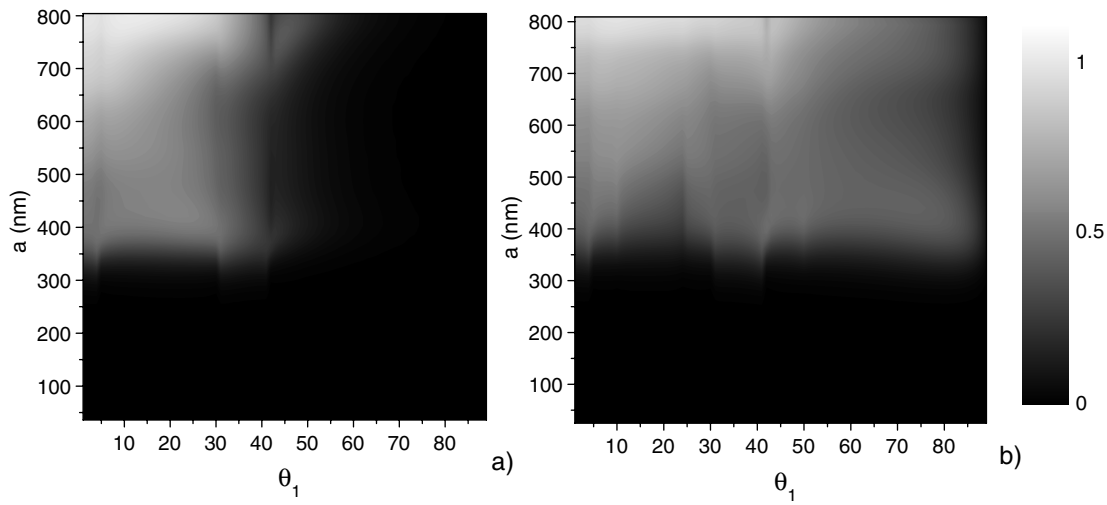

Figure 4. Maps of total transmitted intensity as a function of the incidence angle θ_1 and of the slit width a/λ_0 for a periodic array of rectangular silver wires under s-polarized illumination, $d = 814$ nm, $h = 358$ nm, $\varepsilon_1 = 2.25$, $\lambda_0 = 717$ nm and $\nu_2 = 0.146 + i4.64$. (a) $e = 179.25$ nm; (b) $e = 10$ nm.

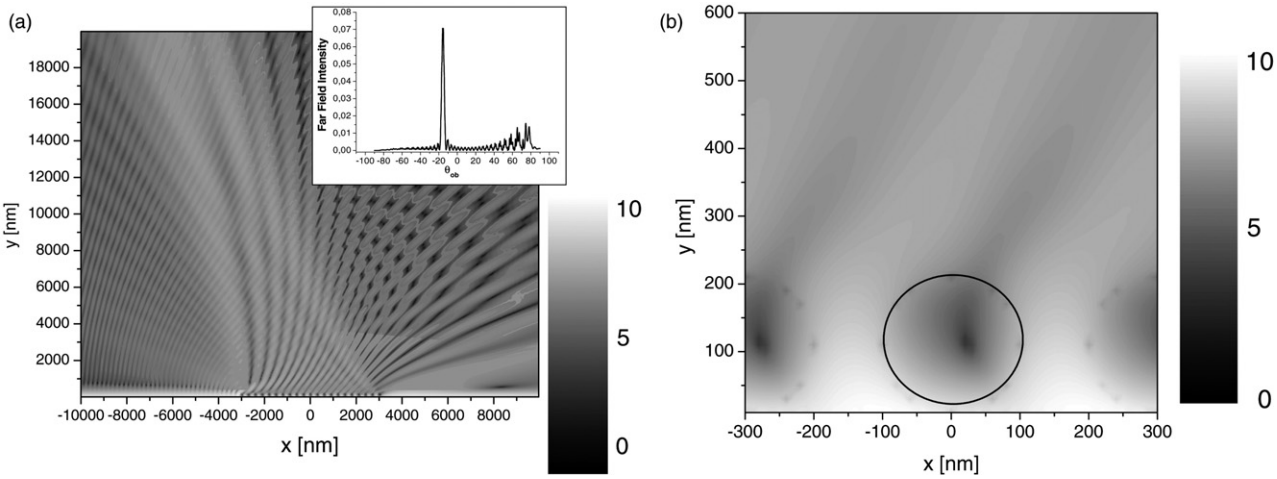

Figure 5. Maps of electric near-field intensity for an array of 21 silver circular wires illuminated by a s-polarized Gaussian beam of half-width $W = 16\lambda_0$, $r = 100$ nm, $d = 300$ nm, $e = 110$ nm (see figure 1(b)), $\varepsilon_1 = 2.25$, $\lambda_0 = 400$ nm. (a) Intensity map (the inset shows the angular distribution of the far-field intensity); (b) detail of the map in (a) near the central cylinder.

enables certain channels in which light can propagate to the far field. The second one is the excitation of FPRs within the slits between adjacent wires. This mechanism produces an intensification of the field within the slits, and consequently can help the coupling, enhancing the transmitted diffraction orders. However, if this second phenomenon is not present, i.e., if no Fabry–Perot resonances are excited in the slits, the propagation channels opened by the periodicity cannot be exploited since there is no enhancement of the field within the slits, producing a very weak field at the further boundary of the array. This is the case of the example shown in figure 5, where we show the intensity map of electric near field (log scale) for a finite array of circular wires. In this system, the geometrical characteristics responsible for the enhancement and the coupling in the infinite system of rectangular wires are no longer present: the infinite structure is now finite (it has 21 cylinders), and the rectangular slits that generate the FPRs now have a different shape, not favourable for the excitation of such resonances. In figure 5 we consider an array of 21 circular silver wires illuminated by a Gaussian beam of half-width $W = 16\lambda_0$, $\lambda_0 = 400$ nm. The parameters of the array are: $d = 0.75\lambda_0$, $r = 0.25\lambda_0$, $e = 0.275\lambda_0$ (see figure 1(b)), $\theta_1 = 45° > \theta_c$.

For these parameters, the smaller size of the cavity between adjacent wires is $a = 0.25\lambda_0$ and only the -1 diffraction order can propagate. The dielectric–air interface is at $y = 0$ and the incident beam impinges on the interface from $y < 0$. Propagating transmitted waves over the array (for $y > e + r$) can be observed for negative observation angles (the zeroth diffraction order is not allowed). Figure 5(b) shows a detail of the intensity map of figure 5(a) around the central wire. It is possible to observe the skin effect and the evanescent electric field through the apertures. The evanescent electromagnetic field propagates through each cavity up to the top of the array, and a set of coherent evanescent sources are obtained. In this way, the coupling mechanism of evanescent to propagating waves is stimulated. It can be observed that, even though the infinite characteristic of the structure is well simulated by just 21 cylinders, i.e. the corresponding transmitted orders are generated, they carry almost no power, since the second mechanism, related to the enhancement of the field within the slits helped by FPRs, is not present for this geometry. The inset in figure 5(a) shows the angular distribution of intensity for the far field. An intensity peak can be observed around $\theta_{\text{obs}} = -15.8°$, which corresponds to the propagating -1 order. The conversion efficiency in this case is poor and no FPR are excited, $T(\theta = 45°) \approx 0.1\%$, as expected for this geometry.

4. Summary and discussion

We have shown that an evanescent electromagnetic wave generated at a dielectric interface can be coupled to a propagating wave by means of a periodic array of metallic wires. In particular, for subwavelength cavities between the wires, evanescent-to-propagating transmission can be achieved even for an incident s-polarized wave. In particular, the enhanced transmission observed in rectangular cavities has been explained in terms of the excitation of Fabry–Perot resonances within the slits, and taking into account the effective refraction index inside the slits. In general, it was found that, when the first mode is propagating, a significant rate of evanescent-to-propagating coupling is obtained, even for very thick wires. Moreover, the efficiency of the coupling increases when the array is closer to the dielectric interface. Even though the existence of this coupling is a consequence of the vicinity of the metallic array to the dielectric interface, regardless of the wires' cross section, we have shown that the coupling efficiency is highly dependent on the wires' geometry, since it is based on Fabry–Perot resonances.

Acknowledgments

The authors gratefully acknowledge partial support from Consejo Nacional de Investigaciones Científicas y Técnicas (CONICET), Universidad de Buenos Aires (UBA), Universidad Nacional de la Provincia de Buenos Aires (UNICEN) and Agencia Nacional de Promoción Científica y Tecnológica (ANPCYT-BID 1728/OC-AR-14099). This work was also supported by a grant of Red Argentina de Optica y Fotofísica.

References

[1] Ebbesen T W, Lezec H J, Ghaemi H F, Thio T and Wolff P A 1998 Extraordinary optical transmission through sub-wavelength hole arrays *Nature* **391** 667–9

[2] Porto J, García-Vidal F J and Pendry J 1999 Transmission resonances on metallic grating with very narrow slits *Phys. Rev. Lett.* **83** 2845–8

[3] Astilean S, Lalanne Ph and Palamaru M 2000 Light transmission through metallic channels much smaller than the wavelength *Opt. Commun.* **175** 265–73

[4] Xie Y, Zakharian A R, Moloney J V and Mansuripur M 2005 Transmission of light through a periodic array of slits in a thick metallic film *Opt. Express* **13** 4485–91

[5] Lee J W, Seo M A, Kim D S, Jeoung S C, Lienau Ch, Kang J H and Park Q-H 2006 Fabry–Perot effects in THz time-domain spectroscopy of plasmonic band-gap structures *Appl. Phys. Lett.* **88** 071114

[6] Skigin D C and Depine R A 2005 Transmission resonances on metallic compound gratings with subwavelength slits *Phys. Rev. Lett.* **95** 217402 (Paper selected for publication in the Virtual Journal of Nanoscale Science and Technology http://www.vjnano.org/nano/ 12, (22) (2005))

[7] Skigin D C and Depine R A 2006 Resonances on metallic compound transmission gratings with subwavelength wires and slits *Opt. Commun.* **262** 270–5

[8] Born M and Wolf E 1999 *Principles of Optics* 7th edn (Cambridge: Cambridge University Press)

[9] Stratton J A 1941 *Electromagnetic Theory* (New York: McGraw-Hill)

[10] Wood R W 1902 On a remarkable case of uneven distribution of light in a diffraction grating spectrum *Phil. Mag.* **4** 396

[11] Maradudin A A, Wallis R F and Dobrzynsky L 1980 *Surface Phonons and Polaritons* (*Handbook of Surfaces and Interfaces* vol 3) (New York: Garland STPM Press)

[12] Raether H 1988 *Surface Polaritons on Smooth and Rough Surfaces and on Gratings* (Berlin: Springer)

[13] Lester M and Depine R 1996 Reflection of electromagnetic waves from index-matched surfaces *Opt. Commun.* **127** 189–92

[14] Pendry J B, Martin-Moreno L and García-Vidal F J 2004 Mimicking surface plasmons with structured surfaces *Science* **305** 847–8

[15] Lester M and Nieto-Vesperinas M 1999 Optical forces on microparticles in an evanescent laser field *Opt. Lett.* **26** 936–8
Lester M, Arias-Gonzlez J R and Nieto-Vesperinas M 2001 Fundamentals and model of photonic-force microscopy *Opt. Lett.* **26** 707–9

[16] Mulin D, Girard C, Colas des Francs G, Spajer M and Courjon D 2000 Near-field optical probing of two-dimensional photonic crystals: theory and experiment *J. Microsc.* **202** 110–6

[17] Fang N, Lee H, Sun C and Zhang X 2005 Sub-diffraction-limited optical imaging with a silver superlens *Science* **308** 534–7

[18] Tetz K A, Rokitski R, Nezhad M and Fainman Y 2005 Excitation and direct imaging of surface plasmon polariton modes in a two-dimensional grating *Appl. Phys. Lett.* **86** 111110

[19] Dintinger J, Klein S, Bustos F, Barnes W L and Ebbesen T W 2005 Strong coupling between surface plasmon-polaritons and organic molecules in subwavelength hole arrays *Phys. Rev.* B **71** 035424

[20] Byun K M, Kim S J and Kim D 2005 Dosing study of highly sensitive nanowire-enhanced surface plasmon resonance biosensors using rigorous coupled wave analysis *Opt. Express* **13** 3737–42

[21] Krishnan A, Thio T, Kim T J, Lezec H J, Ebbesen T W, Wolff P A, Pendry J, Martin-Moreno L and García-Vidal F J 2001 Evanescently coupled resonance in surface plasmon enhanced transmission *Opt. Commun.* **200** 1–7

[22] Vohnsen B and Bozhevolnyi S I 2001 Coupling of surface-plasmon polaritons to directional far-field radiation by and individual surface protrusion *Appl. Opt.* **40** 6081–5

[23] Park S, Lee G, Song S H, Oh C H and Kim P S 2003 Resonant coupling of surface plasmons to radiation modes by use of dielectric gratings *Opt. Lett.* **28** 1870–2

[24] Steele J M, Moran C E, Lee A, Aguirre C M and Halas N J 2003 Metallodielectric gratings with subwavelength slots: optical properties *Phys. Rev.* B **68** 205103

[25] Moreno E, Martin-Moreno L and Garcia-Vidal F J 2006 Extraordinary optical transmission without plasmons: the s-polarization case *J. Opt. A: Pure Appl. Opt.* **8** S94–7

[26] Skigin D C and Lester M 2006 Study of resonant modes of a periodic metallic array near a dielectric interface: evanescent-to-propagating coupling via surface plasmon excitation *J. Opt. A: Pure Appl. Opt.* **8** 259–67

[27] Masoller C, Torre M S and Mandel P 2006 Influence of the injection current sweep rate on the polarization switching of vertical-cavity surface-emitting lasers *J. Appl. Phys.* **99** 026108

[28] Torre M S, Valle A and Pesquera L 2006 Polarization and transverse mode behaviour of VCSELs under optical injection *Opt. Quantum Electron.* **48** 445–65

[29] Torre M S, Masoller C and Mandel P 2006 Transverse and polarization effects in index-guided vertical-cavity surface-emitting lasers *Phys. Rev.* A **74** 043808

[30] Andrewartha J R, Fox J R and Wilson I J 1977 Resonance anomalies in the lamellar grating *Opt. Acta* **26** 69–89

[31] Lochbihler H and Depine R 1993 Diffraction from highly conducting wire gratings *Appl. Opt.* **32** 3459–65

[32] Skigin D C and Depine R A 1998 Scattering by lossy inhomogeneous apertures in thick metallic screens *J. Opt. Soc. Am.* A **15** 2089–96

[33] Maradudin A A, Michel T, McGurn A R and Mendez E R 1990 Enhanced backscattering of light from a random grating *Ann. Phys.* **203** 255–307

[34] Madrazo A and Nieto-Vesperinas M 1995 Scattering of electromagnetic waves from a cylinder in front of a conducting plane *J. Opt. Soc. Am.* A **12** 1298

[35] Gordon R and Brolo A 2005 Increased cut-off wavelength for a subwavelength hole in a real metal *Opt. Express* **13** 1933–8

[36] Gordon R 2006 Light in a subwavelength slit in a metal: propagation and reflection *Phys. Rev.* B **73** 153405